

Electrical characteristics study of heterojunction solar cells CdS/CIGS

H. Amar^{1,2}, M. Amir³, H. Ghodbane², B. Babes^{1*}, M.N. Kateb², M.A. Zidane⁴, A. Rauane⁴

¹Research Center in Industrial Technologies CRTI,

P.O. Box 64, Cheraga 16014 Algiers, Algeria

²University Mohamed Khider of Biskra, Algeria

³University Mouloud Mammeri of Tizi Ouzou, Algeria

⁴University of Lorraine, CNRS, IJL, F-54000 Nancy, France

*Corresponding author e-mail: elect_babes@yahoo.fr

Abstract. In this work, we carried out the study of electrical characteristics with two-dimensional numerical analysis by using the Aided Design (TCAD Silvaco) software for CdS/CuInGaSe₂ (CIGS) thin solar cells. Their structure is composed of a thin CIGS solar cell in the configuration: ZnO(200 nm)/CdS(50 nm)/CIGS (350 nm)/Mo. Then ZnO is used for conductive oxide contacted transparent front of the cell. For rear contact, the molybdenum (Mo) is used. The layer of the CdS window and the shape of the CIGS absorber is the *n-p* semiconductor heterojunction. The performance of the cell was evaluated by applying the defects created in the grain joints of polycrystalline CdS and CIGS material and CIGS/CdS interface in the model, and the physical parameters used in the TCAD simulations have been calibrated to reproduce experimental data. The *J-V* characteristics are simulated under AM1.5 illumination conditions. The conversion efficiency (η) 20.10% has been reached, and the other characteristic parameters have been simulated: the open-circuit voltage (V_{oc}) is 0.68 V, the circuit-current density (J_{sc}) is equal to 36.91 mA/cm², and the form factor (FF) is 0.80. The simulation results showed that the molar fraction *x* of the CIGS layer has an optimal value around 0.31 corresponding to a gap energy of 1.16 eV, this result is in very good agreement with that found experimentally.

Keywords: physical models, TCAD Silvaco, CIGS solar cell, heterojunction.

<https://doi.org/10.15407/spqeo24.04.457>

PACS 73.40.-c, 73.50.Pz, 88.40.hj

Manuscript received 22.03.21; revised version received 14.06.21; accepted for publication 10.11.21; published online 23.11.21.

1. Introduction

Thin-film solar cells have large-scale terrestrial photovoltaic applications due to their low manufacturing price. A number of semiconductors including CdTe polycrystalline, CIGS and amorphous silicon (*a-Si*) have been developed for thin-film solar cells. CIGS-based solar cells have excellent stability and radiation resistance [1, 2]. They have a considerable interest in space applications, proton and electron irradiation tests on solar cells in CIGS and CdTe have shown that their stability against particle irradiation is superior to that of solar cells in Si or III-V semiconductors [3]. CIGS is a semiconductor with an appropriate energy gap and a high optical absorption coefficient in the visible range of solar spectrum. The film absorption coefficient in CIGS is 100 times higher than that of Si in the visible range of solar spectrum. The maximum efficiency of the best CIGS solar cell manufactured on stainless steel substrates is 17.5% under the AM1.5G [4] illumination conditions. The structure of this device is composed as follows: MgF₂/ITO/ZnO/CdS/CIGS/Mo/stainless steel substrate.

The solar cell with CIGS of molar fraction $x = 0.3$ corresponds to the gap energy of 1.1...1.2 eV and being manufactured on glass substrates has a yield of 20% under AM1.5G [5], as reported by the research team of NREL (National Renewable Energy Laboratory). In recent years, advances have resulted in better cells with a CIGS layer between 2.5 and 3 μm thick, and an energy gap in the range between 1.2 and 1.3 eV, exceeding 20% efficiency and reaching a new world record of 20.3% [6]. A numerical simulation study by using the AMPS-1D simulation tool of a solar cell in CdS/CIGS resulted in a maximum efficiency of 19% [7]. The improvement of the efficiency of the solar cell in CIGS is mainly through the use of double solar cells (tandem), triple- or multi-junctions which are composed of layers having different gap energies to exploit the different regions of the energies in solar spectrum. In this work, we will use the Atlas simulator of the TCAD-Silvaco software in the design and study of a solar cell with CIGS. The Atlas tool allows to design and predict the performance of semiconductor devices and solar cells. This work will

contribute to a better understanding and analysis of solar cells based on CIGS. In this study, we will simulate the effect of thickness, doping of CIGS layers and molar fraction x on solar cell photovoltaic parameters.

2. Theoretical

2.1. Diagram of solar cell energy bands in CIGS at thermodynamic equilibrium

The energy band diagram for the CIGS solar cell simulated at thermodynamic equilibrium is shown in Fig. 1.

2.2. Structure of the cell under study

The solar cell studied in this work is a heterojunction ($n-p$) containing the following layers (Fig. 2).

2.3. Physical models and input parameters

The models we used in our simulation are described in the Atlas literature and in the literature [2, 3]. They and are as follows:

- ✓ The Shockley–Read–Hall (SRH) recombination model.
- ✓ The recombination model at the CdS/CIGS interface: the recombination speeds of electrons (holes) S_n (S_p) = 10^5 cm/s.
- ✓ The defect density model: we considered two Gaussian distributions of defects corresponding to donor states in ZnO [4], the acceptor states present in CdS [4] and the acceptor states in CIGS [5].

The parameters of ZnO, CdS and CIGS materials used in the simulated solar cells are reported from [4] and summarized in Table 1. In Table 2, we have the grouped values of the defect density parameters. Where NDG and NAG are the integrated values of the Gaussian distributions. Gaussians are entered at the energies EGA and EGD, respectively. WG is the width of the distribution.

Table 1. Parameters of ZnO, CdS and CIGS materials used in solar cell simulation.

Material Parameters	ZnO	CdS	CIGS
Thickness (μm)	0.2	0.05	3.5
E_g (eV)	3.3	0.05	1.16
N_c (cm^{-3})	$2.2 \cdot 10^{18}$	$2.2 \cdot 10^{18}$	$2.2 \cdot 10^{18}$
N_v (cm^{-3})	$1.8 \cdot 10^{19}$	$1.8 \cdot 10^{19}$	$1.8 \cdot 10^{19}$
Mobility of electrons ($\text{cm}^2/\text{V}\cdot\text{s}$)	25(100)	25(140)	25(140)
Permittivity	9	10	13.6
Electronic affinity (eV)	4.7	4.5	4.8

Table 2. ZnO, CdS and CIGS material defect density parameters.

Material Parameters	ZnO	CdS	CIGS
NDG, NAG (cm^{-3})	D: 10^{17}	A: 10^{15}	A: 10^{15}
EGA, EGD (eV)	Middle of the gap	Middle of the gap	Middle of the gap
WG (eV)	0.1	0.1	0.1
σ_n (cm^2)	10^{-12}	10^{-17}	$2 \cdot 10^{-16}$
σ_p (cm^2)	10^{-15}	10^{-13}	10^{-15}

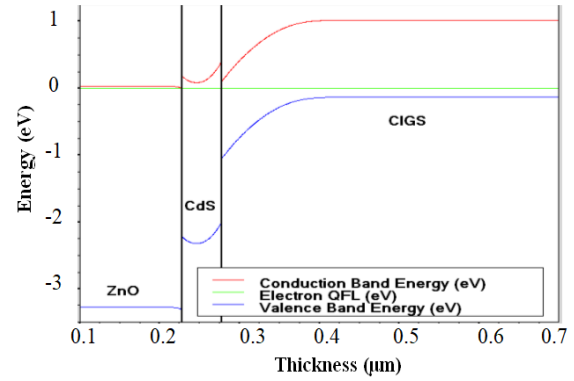


Fig. 1. Diagram of the energy bands of the CIGS solar cell under thermodynamic equilibrium.

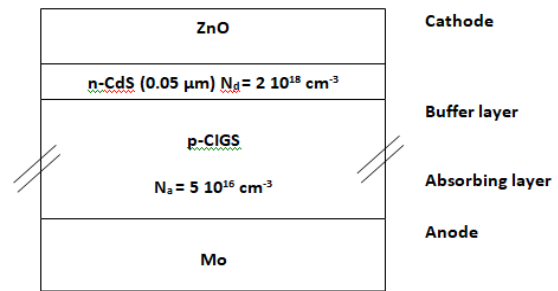


Fig. 2. Structure of the heterojunction solar cell (ZnO/CdS/CIGS).

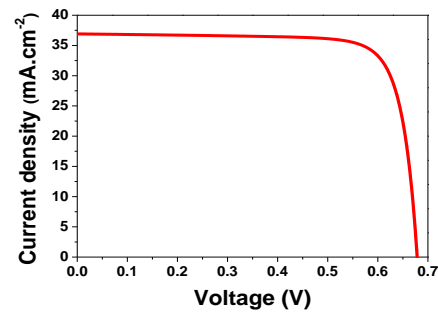


Fig. 3. Characteristic $J(V)$ of the solar cell with the CIGS layer.

3. Results and discussion

3.1. Electrical characteristic of the solar cell

The electrical characteristic ($J-V$) under illumination by the solar spectrum under AM1.5 and power density $100 \text{ mW}/\text{cm}^2$ is shown in Fig. 3. The short-circuit current density $J_{sc} = 36.91 \text{ mA}/\text{cm}^2$, the open-circuit voltage $V_{oc} = 0.68 \text{ V}$, the form factor $\text{FF} = 80\%$ and the conversion efficiency $\eta = 20.1\%$.

We have the possibility to examine the distribution of the rate of photogeneration in the structure under illumination with the solar spectrum AM1.5, and in the short-circuit mode it is represented in Fig. 4. It shows the rate of photogeneration in logarithmic scale as a function of the cell thickness. The results show that the photogeneration rate is maximum at the surface of the solar cell exposed to light, and then it becomes almost constant in the rest of the solar cell.

Table 3. Simulation and experimental parameters of the photovoltaic cell with the CIGS layer.

	J_{sc} (mA·cm ²)	V_{oc} (V)	FF (%)	η (%)
Simulation	36.91	0.68	80	20.1
Experimental	35.4	0.74	77.5	20.3

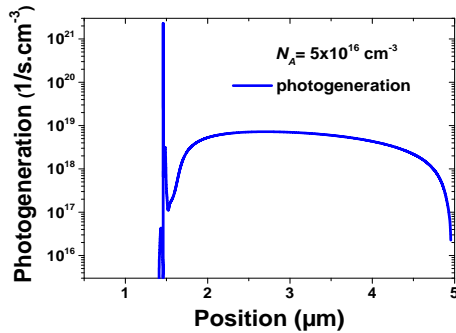


Fig. 4. Photogeneration rate as a function of the thickness of the solar cell ($N_a = 5e^{16}$, $x = 1$ to $5 \mu\text{m}$).

From Fig. 4, we will see that most of the excess carriers are generated in the CIGS absorber, with a less concentration in the vicinity of the surface due to recombination.

3.2. Effect of CIGS layer thickness

We simulated variation of solar cell photovoltaic parameters according to the thickness of the CIGS layer between 0.5 and 5 μm , and the CdS layer is 50 nm. The simulation results are illustrated in Figs 5a to 5d.

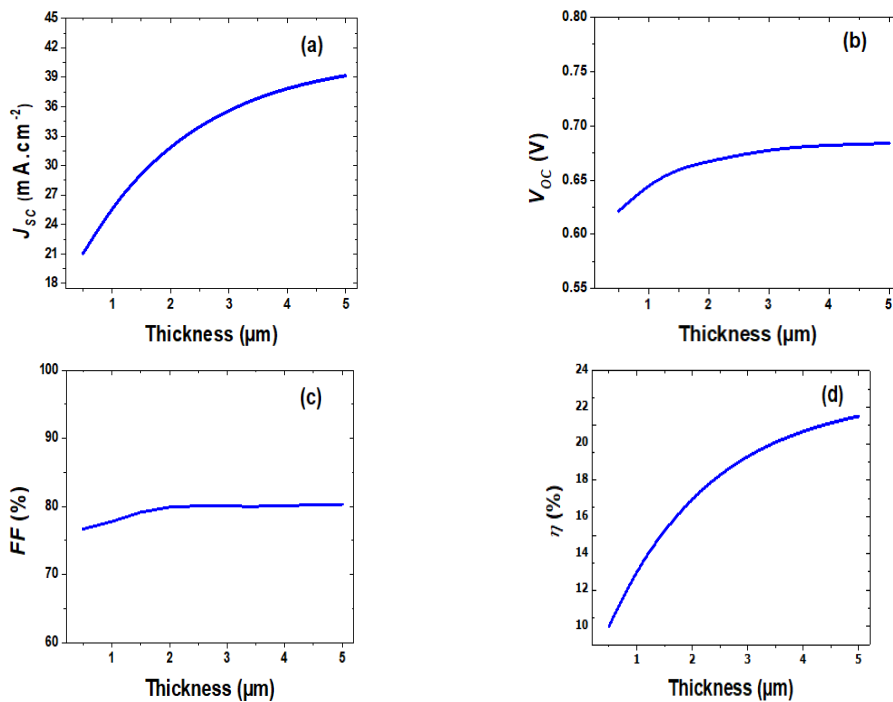


Fig. 5. Variation of solar cell photovoltaic parameters in accord with the thickness of the CIGS layer.

We see an increase in these parameters with increasing the CIGS layer. For the thickness of absorbing layer close to 0.5 μm , the obtained yield is 10%. The highest efficiency found is 21.5%, which corresponds to the thickness 5 μm of the absorbing layer. These results are consistent with simulation results in [8, 9]. The increase in conversion efficiency is mainly due to the increase in the thickness of absorbing layer of p -type in CIGS. As the thickness of this layer increases, more photons with longer wavelengths can be collected in the absorbing layer [10, 11].

As a result, this will contribute to higher generation of electron-hole pairs and, therefore, to increasing the open-circuit voltage and short-circuit current. The increase in V_{oc} and I_{sc} leads to an increase in the conversion efficiency of the solar cell. A very thin absorbing layer physically means that the back contact and the depletion region are very close, which promotes electron capture through this contact. This form of recombination process is detrimental to cell performance, as it affects V_{oc} , J_{sc} and conversion efficiency.

3.3. Effect of CIGS layer doping

The effect of doping the CIGS layer (3.5 μm) on the cell's photovoltaic parameters was simulated using the doping concentration values within the range $2 \cdot 10^{15}$ to 10^{18}cm^{-3} . The concentration of CdS doping N_d (50 nm) was $2 \cdot 10^{18} \text{cm}^{-3}$.

The photovoltaic characteristics have been illustrated in Figs 6a to 6d. The concentration of CIGS absorbing layer doping systematically influences J_{sc} , V_{oc} and FF. In particular, a maximum of the yield $\eta = 21.5\%$,

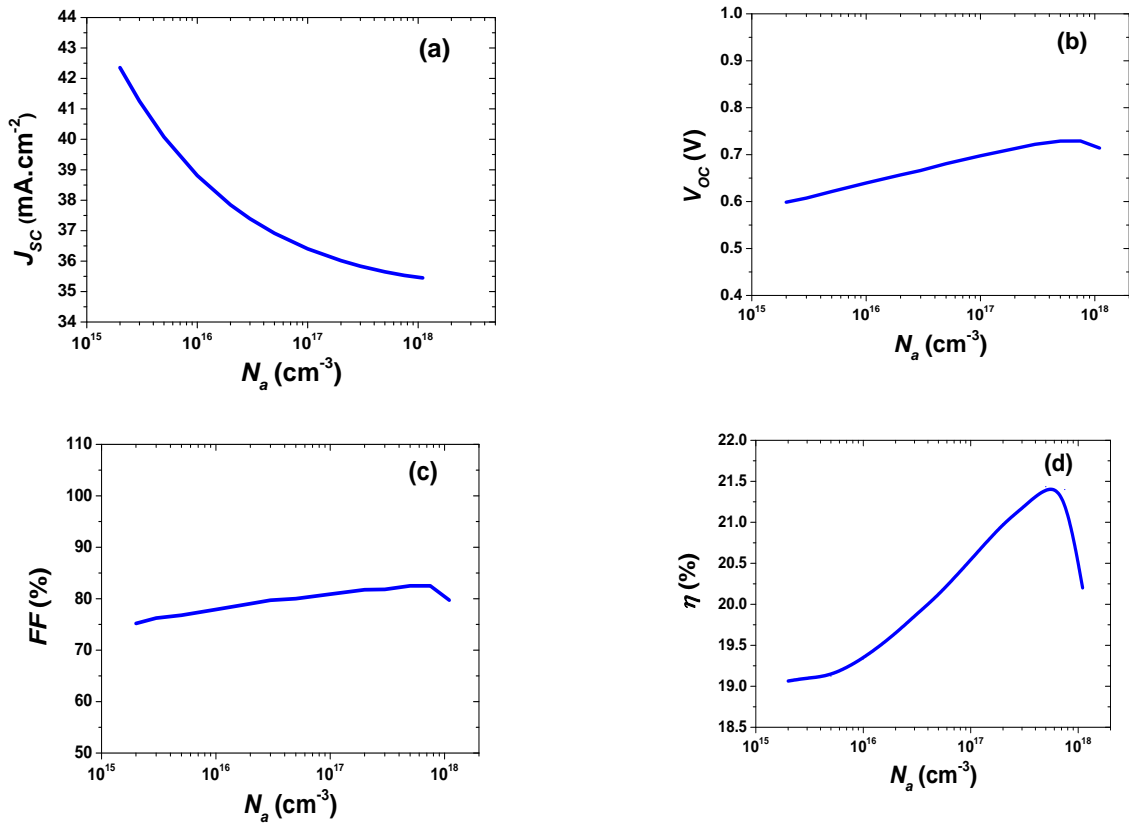


Fig. 6. Variation of solar cell photovoltaic parameters in accord with the thickness of CIGS layer.

the open-circuit voltage and the form factor occurs for the concentration of doping of the order of $5 \cdot 10^{17} \text{ cm}^{-3}$.

According to the figure, there is a rapid decrease in short-circuit current density with the increase in doping the CIGS layer, this is caused by the increase in recombination rate inside the CIGS [12] layer with doping as shown in Fig. 7. This effect of doping was also obtained in [10].

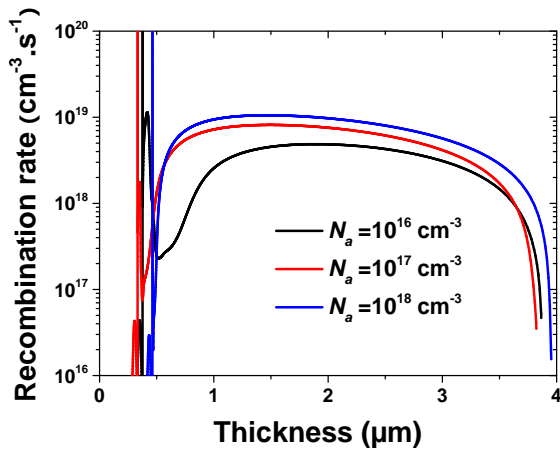


Fig. 7. Recombination rate in the structure for different values of the doping concentration N_a in the CIGS layer.

3.4. Effect of Ga molar fraction in $\text{CuIn}_{1-x}\text{Ga}_x\text{Se}_2$

The quaternary compound $\text{CuIn}_{1-x}\text{Ga}_x\text{Se}_2$ (CIGS) is characterized by a forbidden band that varies with the composition in Ga. The molar fraction $x = \text{Ga}/(\text{Ga}+\text{In})$ changes the bandwidth (gap) according to the following equation [13]:

$$E_g(x) = 1.010 + 0.626x - 0.167x(1-x). \quad (1)$$

Table 4 shows the change in gap energy as a function of x .

In our simulation model, we used experimental measurements of the density of defects as a function of the molar fraction in CIGS performed by Hanna *et al.* [14]. We took into consideration the increase in the defect density of the CIGS layer with the molar fraction x (Fig. 8).

Table 4. The gap energy as a function of x .

Composition x	Gap energy (eV)
0	1.01
0.31	1.15
0.45	1.25
0.66	1.38
1	1.63

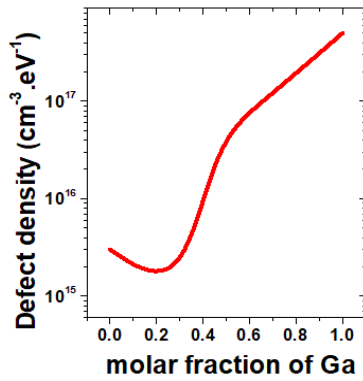


Fig. 8. Change in defect density as a function of the molar fraction x of Ga used in solar cell modeling in CIGS.

The density of defects is $3 \cdot 10^{15} \text{ cm}^{-3} \text{ eV}^{-1}$ for $x = 0$ and then decreases to $1.8 \cdot 10^{15} \text{ cm}^{-3} \text{ eV}^{-1}$ for $x = 0.2$. From this value, the defect density increases to $5 \cdot 10^{17} \text{ cm}^{-3} \text{ eV}^{-1}$ for $x = 1$.

Fig. 9 shows the $J(V)$ characteristics for five molar fraction values taking into account the dependence of the CIGS defect density on x (Fig. 8).

We note that the main effect of increasing x (the gap) of the CIGS layer is in the growth of the open-circuit voltage and decreasing the short-circuit current. The increase in the width of the gap enhances the open-circuit voltage that reaches the value 0.88 V for $x = 1$,

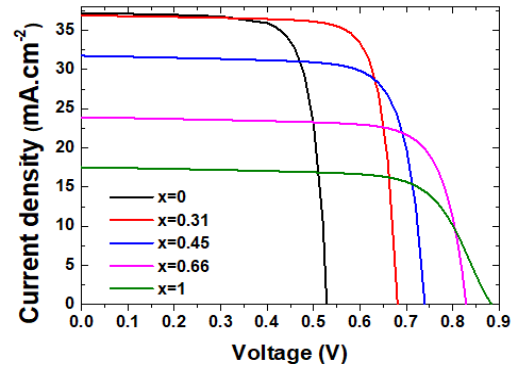


Fig. 9. Characteristics $J(V)$ as a function of the molar fraction x of Ga.

while there is a decrease in the short-circuit current caused by reducing the number of photons absorbed.

The solar cell photovoltaic parameters as a function of the molar fraction x are shown in Fig. 10. The yield increases with x , starting from $x = 0.31$, the yield decreases down to 11% at $x = 1$. A high Ga x composition corresponding to a high density of defects causes a drop in the short-circuit current and subsequent solar cell efficiency. Noting that the optimum value of the yield 20.1% at $x = 0.31$ corresponding to a gap energy of the order of 1.16 eV is in very good agreement with that measured [7, 15].

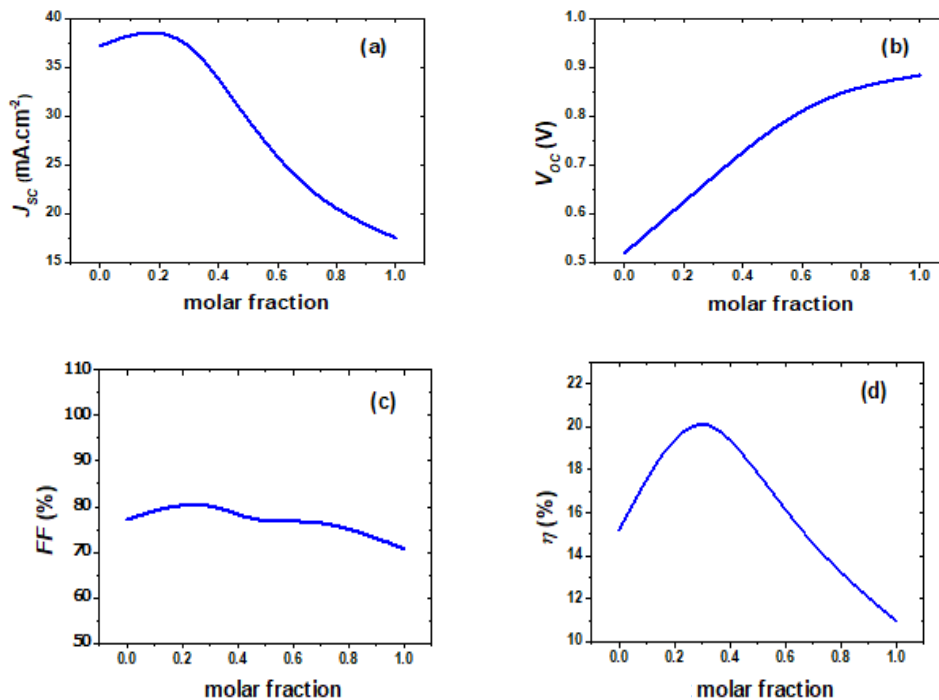


Fig. 10. Variation of solar cell photovoltaic parameters as a function of the molar fraction x .

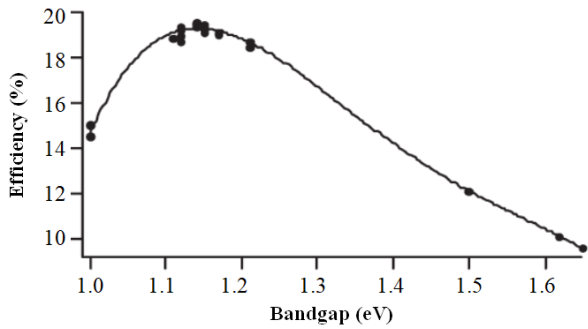


Fig. 11. Efficiency as a function of the energy gap of the CIGS layer.

The energy efficiency of the experimental gap [16] is shown in Fig. 11. The energy of the optimal gap is ~1.15 eV, which is in very good agreement with that we obtained by simulation.

3.5. Effect of the ZnO window layer: Al on the solar cell in CIGS

CIGS solar cells use an Al-doped (ZnO:Al) ZnO layer more frequently. A combination of an intrinsic layer (ZnO) and a doped layer (ZnO:Al) is generally used because this double layer promotes higher yields [17]. So in our study, we simulated the effect of the ZnO:Al window layer (300 nm) and the ZnO and ZnO:Al double layer (500 nm). The structures of the two solar cells are shown in Fig. 12. The doping thickness and concentration of the two layers in CdS and CIGS are as shown in Table 3.

The electrical characteristics $J(V)$ of three solar cells with CIGS; the first with a window layer of ZnO, the second with a window layer of ZnO:Al, and the third with a double layer of ZnO and ZnO:Al are shown in Fig. 13.

The photovoltaic parameters J_{sc} , V_{oc} , FF, and η of the three solar cells are grouped in Table 5.

Being based on these results, we note that the efficiency of the solar cell with the double window layer

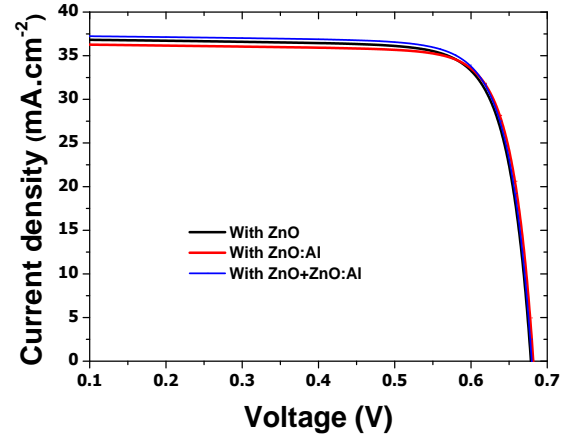


Fig. 13. Characteristics $J(V)$ of three solar cells with CIGS; the first with a window layer of ZnO, the second with a window layer of ZnO:Al, and the third – with a double layer of ZnO and ZnO:Al.

Table 5. Photovoltaic parameters.

	FF (%)	V_{oc} (V)	J_{sc} (mA·cm ⁻²)	η (%)
ZnO	80	0.68	36.91	20.1
ZnO:Al	81.38	0.68	36.36	20.21
ZnO:Al + ZnO	80.06	0.68	37.33	20.37

of ZnO and ZnO:Al is higher than that with the window layer of ZnO or ZnO:Al only, it increases from 20.1 up to 20.37%. The improvement of the efficiency of the solar cell in CIGS by using the double window layer in ZnO and ZnO:Al is related to the improvement of the conductivity of the ZnO:Al [18] layer by the doping with Al and the decrease of its serial resistance. Increased Al doping concentration affects the optical gap, and ZnO conductivity increases [6, 19]. The ZnO:Al layer has a high transparency in the visible range, it is characterized by a high optical transmission, which allows the efficient transport of photons to the active CIGS layer [20, 21].

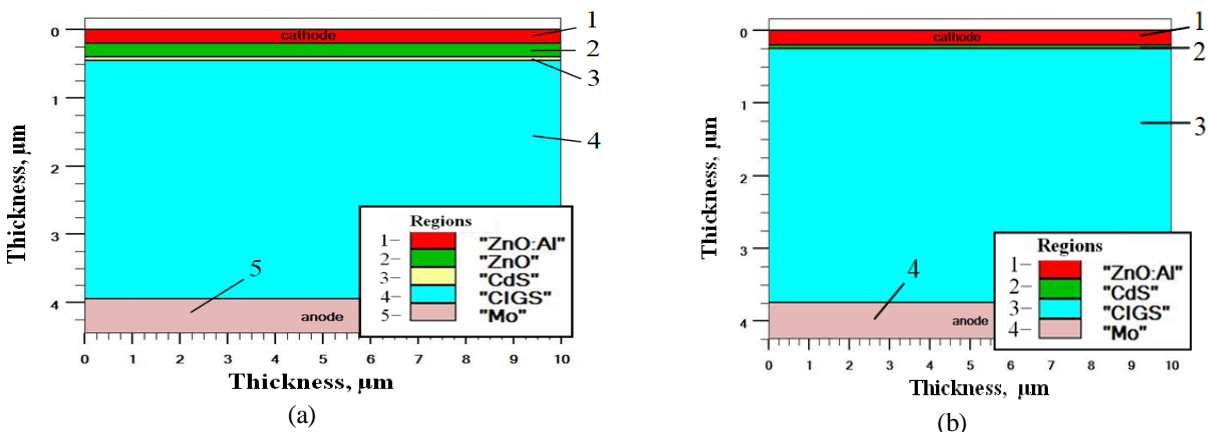


Fig. 12. (a) Structure with ZnO:Al, (b) structure with ZnO + ZnO:Al.

4. Conclusion

The numerical simulation of the solar cell allowed us to calculate the photovoltaic parameters that characterize the solar cell. The values of these photovoltaic parameters are as follows: the short-circuit current density $J_{sc} = 36.91 \text{ mA/cm}^2$, the open-circuit voltage $V_{oc} = 0.68 \text{ V}$, the form factor $FF = 80\%$, and the conversion efficiency $\eta = 20.1\%$. These values are in very good agreement with those found experimentally.

We then studied the sensitivity of the photovoltaic parameters of the solar cell to the dimensions (thickness, doping) of the CIGS layer of p -type and the molar fraction x of CIGS. We observed an increase in photovoltaic parameters, when the thickness of the CIGS layer increases. The highest found efficiency is 21.5%, which corresponds to the thickness close to $5 \mu\text{m}$. The concentration of the CIGS absorbing layer doping systematically influences the photovoltaic parameters. There is a rapid drop in short-circuit current density with doping. In particular, the maximum efficiency $\eta = 21.5\%$, the open-circuit voltage and the form factor occur for the concentration of doping close to $5 \cdot 10^{17} \text{ cm}^{-3}$. An improvement in the performance inherent to the solar cell with CIGS has been reached by addition of the ZnO:Al window layer.

References

1. Manual, A. U. S. Device Simulation Software version 5.19. 17. C (*Silvaco International, Santa Clara, CA, USA*), 2013.
2. Bouloufa A., Djessas K., and Zegadi A. Numerical simulation of $\text{CuIn}_x\text{Ga}_{1-x}\text{Se}_2$ solar cells by AMPS-1D. *Thin Solid Films*. 2007. **515**. P. 6285–6287. <https://doi.org/10.1016/j.tsf.2006.12.110>.
3. Mezghache M., Hadjoudja B. Improved performance in bilayer-CIGS solar cell. *International Renewable and Sustainable Energy Conference (IRSEC)*. 2013. P. 82–85. <https://doi.org/10.1109/IRSEC.2013.6529693>.
4. Gloeckler M., Fahrenbruch A.L. and Sites J.R. Numerical modeling of CIGS and CdTe solar cells: setting the baseline. *3rd World Conference on Photovoltaic Energy Conversion, 2003. Proc.* 2003. **1**. P. 491–494. <https://doi.org/10.1109/WCPEC.2003.1305328>.
5. Song S.H., Nagaich K., Aydil E.S. *et al.* Structure optimization for a high efficiency CIGS solar cell. *35th IEEE Photovoltaic Specialists Conference*. 2010. P. 2488–2492. <https://doi.org/10.1109/PVSC.2010.5614724>.
6. Richter M., Schubert C., Eraerds P. *et al.* Optical characterization and modeling of $\text{Cu}(\text{In}, \text{Ga})(\text{Se}, \text{S})_2$ solar cells with spectroscopic ellipsometry and coherent numerical simulation. *Thin Solid Films*. 2013. **535**. P. 331–335. <https://doi.org/10.1016/j.tsf.2012.11.078>.
7. Jackson P., Hariskos D., Lotter E. *et al.* New world record efficiency for $\text{Cu}(\text{In}, \text{Ga})\text{Se}_2$ thin film solar cells beyond 20%. *Progress in Photovoltaics: Research and Applications*. 2011. **19**. P. 894–897. <https://doi.org/10.1002/pip.1078>.
8. Chelvanathan P., Hossain M.I., Amin N. Performance analysis of copper–indium–gallium–diselenide (CIGS) solar cells with various buffer layers by SCAPS. *Current Applied Physics*. 2010. **10**. P. S387–S391. <https://doi.org/10.1016/j.cap.2010.02.018>.
9. Amin N., Chelvanathan P., Hossain M.I., Sopian K. Numerical modelling of ultra thin $\text{Cu}(\text{In}, \text{Ga})\text{Se}_2$ solar cells. *Energy Procedia*. 2012. **15**. P. 291–298. <https://doi.org/10.1016/j.egypro.2012.02.034>.
10. Song J., Anderson T.J., Li S.S. Material parameter sensitivity study on CIGS solar cell performance. *33rd IEEE Photovoltaic Specialists Conf.* 2008. P. 1–4. <https://doi.org/10.1109/PVSC.2008.4922545>.
11. Movla H. Optimization of the CIGS based thin film solar cells: Numerical simulation and analysis. *Optik*. 2014. **125**. P. 67–70. <https://doi.org/10.1016/j.ijleo.2013.06.034>.
12. Hultqvist A., Li J.V., Kuciauskas D. *et al.* Reducing interface recombination for $\text{Cu}(\text{In}, \text{Ga})\text{Se}_2$ by atomic layer deposited buffer layers. *Appl. Phys. Lett.* 2015. **107**. P. 033906. <https://doi.org/10.1063/1.4927096>.
13. Hegedus S.S., Luque A. *Status, Trends, Challenges and the Bright Future of Solar Electricity from Photovoltaics*. Handbook of Photovoltaic Science and Engineering. 2003. P. 1–43. <https://doi.org/10.1002/0470014008.ch1>.
14. Hanna G., Jasenek A., Rau U., Schock H.W. Influence of the Ga-content on the bulk defect densities of $\text{Cu}(\text{In}, \text{Ga})\text{Se}_2$. *Thin Solid Films*. 2001. **387**. P. 71–73. [https://doi.org/10.1016/S0040-6090\(00\)01710-7](https://doi.org/10.1016/S0040-6090(00)01710-7).
15. Contreras M.A., Mansfield L.M., Egaas B. *et al.* Wide bandgap $\text{Cu}(\text{In}, \text{Ga})\text{Se}_2$ solar cells with improved energy conversion efficiency. *Progress in Photovoltaics: Research and Applications*. 2012. **20**. P. 843–850. <https://doi.org/10.1002/pip.2244>.
16. Contreras M.A., Ramanathan K., AbuShama J. *et al.* Accelerated publication: Diode characteristics in state of the art $\text{ZnO}/\text{CdS}/\text{Cu}(\text{In}_{1-x}\text{Ga}_x)\text{Se}_2$ solar cells. *Progress in Photovoltaics: Research and Applications*. 2005. **13**. P. 209–216. <https://doi.org/10.1002/pip.626>.
17. Ishizuka S., Sakurai K., Yamada A. *et al.* Fabrication of wide-gap $\text{Cu}(\text{In}_{1-x}\text{Ga}_x)\text{Se}_2$ thin film solar cells: a study on the correlation of cell performance with highly resistive $i\text{-ZnO}$ layer thickness. *Solar Energy Materials and Solar Cells*. 2005. **87**. P. 541–548. <https://doi.org/10.1016/j.solmat.2004.08.017>.
18. Nishimura T., Hamada N., Chantana J. *et al.* Application of two-dimensional MoSe_2 atomic layers to the lift-off process for producing light-weight and flexible bifacial $\text{Cu}(\text{In}, \text{Ga})\text{Se}_2$ solar cells. *ACS Applied Energy Materials*. 2020. **3**. P. 9504–9508. <https://doi.org/10.1021/acsaem.0c01557>.

19. Elbar M., Tobbeche S., Merazga A. Effect of top-cell CGS thickness on the performance of CGS/CIGS tandem solar cell. *Solar Energy*. 2015. **122**. P. 104–112. <https://doi.org/10.1016/J.SOLENER.2015.08.029>.
20. Elbar M., Tobbeche S. Numerical simulation of CGS/CIGS single and tandem thin-film solar cells using the Silvaco-Atlas software. *Energy Procedia*. 2015. **74**. P. 1220–1227. <https://doi.org/10.1016/j.egypro.2015.07.766>.
21. Yamamoto Y., Saito K., Takahashi K., Konagai M. Preparation of boron-doped ZnO thin films by photo-atomic layer deposition. *Solar Energy Materials and Solar Cells*. 2001. **65**. P. 125–132. [https://doi.org/10.1016/S0927-0248\(00\)00086-6](https://doi.org/10.1016/S0927-0248(00)00086-6).

Authors and CV



Hichem Amar, he received the Engineering degree in 2011 from Mohamed Khider Biskra University of Algeria. In 2014, he received the Magister degree in the field of Signals and Communications. In 2020, he received the PhD degree in the field of Signals and Commu-

nications in Biskra University, Algeria. Class B research master in Industrial Technologies Research Center CRTI: Algiers, DZ Research master. His research interests include: antenna and RF design, NDT by microwave, solar cells, simulation.

E-mail: h.amar@crti.dz;

<https://orcid.org/0000-0002-1713-1491>.



Mounir Amir, born in 1980. He received the MS and PhD degrees in Electronics Engineering from University of Batna, Algeria, in 2007 and 2014, respectively. Currently, he is an Associate Professor in the Department of Electronics Engineering at Mouloud Mammeri University of Tizi-Ouzou,

Algeria. E-mail: mounir.amir@yahoo.fr;

<https://orcid.org/0000-0003-3593-7154>.



Badreddine Babes, born in 1980, he received his BS, MS, and PhD degrees in Electrical Engineering from the University of Setif-1, Algeria, in 2004, 2010, and 2018, respectively. Since 2017, he was with the Research Center in Industrial Technologies (CRTI), Algeria.

His current research interests include predictive control of linear and nonlinear systems applied to motor drives and renewable energy systems, and pulse current control of gas metal arc welding (GMAW) processes.

E-mail: b.babes@crti.dz;

<https://orcid.org/0000-0002-9256-2021>.



Hatem Ghodbane, born in 1972. He received his PhD degree in Electronics Engineering from the University of Mohamed Khider, Biskra, Algeria, in 2012. Currently, he is an Associate Professor in the Department of Electrical Engineering at Mohamed Khider University

of Biskra, Algeria. E-mail: h.ghodbane@univ-biskra.dz



Mohamed Nadjib Kateb, he received the MS degree in 2011 from Mohamed Khider Biskra University of Algeria. He is presently working towards his PhD degree in Electronics Engineering at the same university. His current

research interests include the microelectronics and microwave devices. E-mail: nadjibm3@gmail.com



Mohamed Amine Zidane, received the State Engineering degree in 2015 from the Ecole Nationale Polytechnique (ENP) of Algiers, Algeria and the MS degree in embedded electronic from the University of Lorraine, France, in 2016, and the PhD degree in the

field of electronic systems from the same university in 2019. Since 2020, he is temporary lecturer at the department of Electrical Engineering at the faculty of science and technology. Zidane is interested in the following research areas: sensing technology applied to the measurements of human, electromagnetic, electronics, instrumentation and measurement, antenna design.

E-mail: zidanemohamedamine@gmail.com;

<https://orcid.org/0000-0001-9806-4173>.



Amar Rouane, born in 1955. After obtaining his BS and MS degrees at Ecole Polytechnique of Algiers, he obtained his PhD in Instrumentation and Microelectronics in 1993 at Laboratory of Electronic Instrumentation of Nancy, France. He was employed there as an instructor in 1992, next as Assistant Professor

in 1994 and Professor since 2004. From 1988 till 2012 he makes his research at the Laboratory of Electronic Instrumentation of Nancy in the biomedical field. M. Rouane is member of Jean Lamour Institute since 2013. He is interested in sensing technology applied to the measurement of human, electromagnetics, instrumentation and measurement and electromagnetic modeling.

E-mail: amar.rouane@univ-lorraine.fr;

<https://orcid.org/0000-0001-6290-1267>.

Дослідження електричних характеристик сонячних елементів з гетеропереходом CdS/CIGS

Н. Amar, М. Amir, Н. Ghodbane, В. Babes, М.Н. Kateb, М.А. Zidane, А. Rauane

Анотація. У роботі проведено дослідження електричних характеристик двовимірним чисельним аналізом за допомогою програмного забезпечення Aided Design (TCAD Silvaco) для тонких сонячних елементів CdS/CuInGaSe₂ (CIGS). Структура складається з тонкого сонячного елемента CIGS у конфігурації: ZnO (200 нм)/CdS (50 нм)/CIGS (350 нм)/Mo. Потім ZnO використано для провідного оксиду у контакті з прозорою передньою частиною елемента. Для зворотного контакту використовується молибден (Mo). Шар вікна CdS і форма поглиначка CIGS – це напівпровідниковий *n-p* гетероперехід. Продуктивність елемента оцінювалась з урахуванням кількості дефектів, утворених поблизу стиків полікристалічного матеріалу CdS і CIGS біля інтерфейсу CdS/CIGS у моделі, а фізичні параметри для TCAD моделювання було відкалібровано з метою відтворення експериментальних даних. *J-V* характеристики моделюються за умови освітлення AM1.5. Ефективність перетворення (η) досягає 20,10%. Також моделюються інші характерні параметри: напруга розімкнутого контуру (V_{oc}) дорівнює 0,68 В, густина струму контуру (J_{sc}) дорівнює 36,91 мА/см² та форм-фактор (FF) становить 0,80. Результати моделювання показали, що молярна частка x шару CIGS має оптимальне значення близьке до 0,31, що відповідає енергії забороненої зони 1,16 еВ, це дуже добре узгоджується з експериментальними значеннями.

Ключові слова: фізичне моделювання, програмне забезпечення TCAD Silvaco, CIGS сонячний елемент, гетероперехід.